Available online at www.sciencedirect.com

ScienceDirect

Journal of Solid State Chemistry 180 (2007) 2493–2499

JOURNAL OF SOLID STATE CHEMISTRY

www.elsevier.com/locate/jssc

Quantum efficiency of double activated $Tb_3Al_5O_{12}$:Ce^{3+}, Eu^{3+}

Mihail Nazarov[a,b,*], Do Young Noh[a], Jongrak Sohn[c], Chulsoo Yoon[c]

[a]*Department of Materials Science and Engineering, Gwangju Institute of Science and Technology, 1Oryong-dong, Buk-gu, Gwangju 500-712, Republic of Korea*

[b]*Institute of Electronic Engineering and Industrial Technologies, Academy Sciences of Moldova, Republic of Moldova*

[c]*Samsung Electro-Mechanics Co, Ltd., Metan 3-Dong, Yeogtong-Gu, Suwon, Republic of Korea*

Received 11 April 2007; received in revised form 8 June 2007; accepted 22 June 2007
Available online 1 July 2007

Abstract

The quantum efficiency and luminescence properties of double activated terbium aluminum garnet samples were investigated in the present study. A mathematical procedure and PL measurement system are developed for express analysis of quantum efficiency of luminescent materials. The energy-level diagram was proposed to explain the luminescence mechanism. Application of TAG:Ce,Eu with improved CIE and CRI in LED device is demonstrated.

PACS: 78.55.−m

Keywords: Optical materials; Quantum efficiency; Photoelectron spectroscopy; Luminescence

---

1. Introduction

The development of wide band gap III–V nitride compound semiconductors has led to the commercial production of high-efficiency LEDs [1,2]. The recent advent of blue InGaN technology has made it possible to produce a conventional white LED in which white light is obtained by coating a $Y_3Al_5O_{12}$:Ce (YAG) or $Tb_3Al_5O_{12}$:Ce (TAG) phosphor onto a blue LED chip [3–5]. In this device, known as a two-band white LED, white light is generated by additive color mixing of the blue light emitted by the blue LED and the yellow light emitted by the YAG or TAG phosphors. However, the spectral composition of the light produced by the conventional two-band white LED differs from that of natural white light, particularly in the red region. To improve the color properties of the device there are two different ways. First of them is based on adding another component to create a white LED with three emission bands (a three-band white LED). Blue LEDs have been combined with phosphors to convert part of the blue light to red and green light, to produce white light [6]. In this study we propose other way by double activation TAG phosphor with rare-earth (RE) elements. RE phosphors can be separated into two types: broad band emitting owing to the 5*d*–4*f* transition (Eu^{2+}, Ce^{3+}) or narrow band emitting owing to the transition between the 4*f* levels (Eu^{3+}, Tb^{3+}, Sm^{3+}). For white light in blue LED the broad band emitting phosphors are preferred. Our results of co-doping TAG:Ce^{3+} with Eu^{3+} are presented in this contribution.

To determine or estimate the quantum efficiency (QE) of investigated materials we need in a simple and accurate experimental method. Ideally, such a technique for express analysis should require minimal sample preparation and should be simple in application. In this paper we report a technique that satisfies these criteria.

2. Experimental

2.1. Materials

The powder samples were prepared by a conventional solid-state reaction. According to the nominal composition of $Tb_3Al_5O_{12}$:Ce, Eu, the starting materials Tb_4O_7, Al_2O_3,

---

[*] Corresponding author. Fax: +82 62 970 2304.
E-mail addresses: nazarov@gist.ac.kr, mvnazarov@mail.ru (M. Nazarov).

0022-4596/$ - see front matter © 2007 Elsevier Inc. All rights reserved.
doi:10.1016/j.jssc.2007.06.021

CeO_2 and Eu_2O_3 (99% for Al_2O_3, 99.9% for all other oxides) were weighed and milled. Synthesis took place in a furnace heated by induction using a sealed alumina tube in a reducing atmosphere of H_2/N_2 to stabilize the Tb^{3+} state. The crucible was made out of Al_2O_3. BaF_2, LiF and H_3BO_3 as flux materials were used. The synthesis lasted approximately 2 h at temperature of about 1500 °C. The samples were prepared with different Ce (1, 3 and 5 mol%) and Eu (1, 3, 5, 7, 9, 11 and 13 mol%) concentrations.

2.2. Methods

Phosphor samples were characterized by crystalline structure and luminescence properties. Particle sizes and morphologies of the investigated phosphors were determined by scanning electron microscope (SEM) Hitachi-S-3000N. To control the particle size and to find the size distribution the laser diffraction was carried out using HELOS particle size analysis system. The crystal structure and the composition of powder samples were characterized by X-ray diffraction using an X-ray diffractometer D/max–RC, Rigaku, Japan with CuKα radiation ($4\lambda = 1.54056$ A).

Optical spectroscopy and PL characteristics were estimated on the basis of emission and excitation spectra registered at room temperature (Xe 500 W lamp) with DARSA PRO 5100 PL System (Professional Scientific Instrument Co, Korea). Excitation spectra were corrected for the energy distribution of the Xe-lamp. The excitation was performed with a 460 nm radiation, which is usually used in blue LED, as well as with selectively excited emission to establish the luminescence mechanism in cerium–europium double activated terbium aluminum garnet phosphor.

Emission, excitation, and reflection spectra have to be measured for calculation the quantum efficiency of phosphors. The QE of a luminescent material is defined as the ratio of the number of photons emitted to the number of photons absorbed. Two monochromators and Xe lamp as excitation source are necessary. $(YGd)_3Al_5O_{12}$:Ce (YAG) phosphor with known QE could be proposed as standard test sample. If the spectroscopic system does not have a special integrated sphere (ISO40-SF/IG, for example), and does not allow to measure the guantum efficiency directly, the reflectance spectra measurements have to be carried out.

Spectral photon irradiance is expressed as:

$$E^*_\mathrm{p}(\lambda) = \frac{\mathrm{d}E_\mathrm{p}}{\mathrm{d}\lambda}, \quad E_\mathrm{p} = \int_0^\infty E^*_\mathrm{p}(\lambda)\,\mathrm{d}\lambda. \tag{1}$$

For quantum efficiency of investigated sample and standard one we have:

$$\frac{\alpha_\mathrm{x} q_\mathrm{x}}{\alpha_\mathrm{st} q_\mathrm{st}} = \frac{E_{\mathrm{p_x}}}{E_{\mathrm{p_{st}}}}, \tag{2}$$

where q_x and q_st are the quantum efficiencies of the specimen investigated and the standard (commercial YAG material, for example), and α is an absorption coefficient

$$q_\mathrm{x} = \frac{(1 - R_\mathrm{st}) \int_0^\infty E^*_\mathrm{px}(\lambda)\,\mathrm{d}\lambda}{(1 - R_\mathrm{x}) \int_0^\infty E^*_\mathrm{pst}(\lambda)\,\mathrm{d}\lambda} q_\mathrm{st}. \tag{3}$$

The following formula is applied in the calculations:

$$q_\mathrm{X} = \frac{(1 - R_\mathrm{ST})}{(1 - R_\mathrm{X})} \frac{\Phi_\mathrm{X}}{\Phi_\mathrm{ST}} q_\mathrm{ST}, \tag{4}$$

where R_X and R_ST are the reflectance of the specimen and the standard, and Φ_X and Φ_ST are the total measured luminescence efficiency (the integrated area under the emission spectrum) of the specimen and the standard, respectively.

The reflectance R_X and R_ST, respectively, of the investigated and standard samples are calculated from the formula

$$R_\mathrm{N} = \frac{A_\mathrm{RN}}{A_\mathrm{RB}} 0.97, \tag{5}$$

where R_N stands for a sample reflectance ($N = \mathrm{X}$ and ST for investigated powders and the YAG standard, respectively), and A_RN and A_RB are total areas under the measured reflection spectra for the sample investigated and the MgO, respectively. In this formula the number 0.97 represents the reflectance of the MgO powder. (Instead of MgO, $BaSO_4$ with index 0.91 can be used.)

In Fig. 1 we show the scheme of experiment, which is realized with photoluminescent DARSA system for reflectance measurements.

Two monochromators are needed to be synchronized at the excitation wavelength. At the fixed excitation wavelength of the first monochromator the emission spectra around this wavelength are measured by the second monochromator for the reference sample (MgO) and examined phosphors. Because of the Stokes shift (phosphors emit the light at the other wavelength that excites) the measured spectra are the reflectance spectra. The emission and excitation spectra of examined and standard samples are also registered by traditional methods.

3. Results and discussion

Fig. 2 compares excitation and emission spectra of investigated sample $Tb_3Al_5O_{12}:Ce^{3+}$ (TAG) and one of double activated $Tb_3Al_5O_{12}:Ce^{3+}$, Eu^{3+} with commercial $(YGd)_3Al_5O_{12}:Ce^{3+}$ (YAG).

It is seen from Fig. 2 that the luminescence spectra of specimens are very similar in the shape and varies in intensities. The two broad bands from 310 to 380 nm in the long-wavelength UV region and from 400 to 520 nm in the blue spectral region correspond to the 4*f*–5*d* transitions of Ce^{3+} in YAG and TAG [7,8]. Two weak peaks around 375 nm coincide *f*–*f* transition of Tb^{3+}. We can do this conclusion because the same activator Ce^{3+} was introduced in the two different host lattices YAG (1) and TAG (2,3). Only in the TAG we observe these weak peaks. Batentschuk et al. [9] ascribe this due to the absorption by

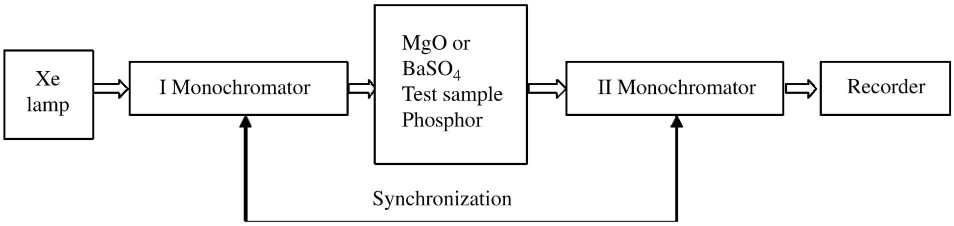

Fig. 1. The scheme of QE measurement with DARSA system.

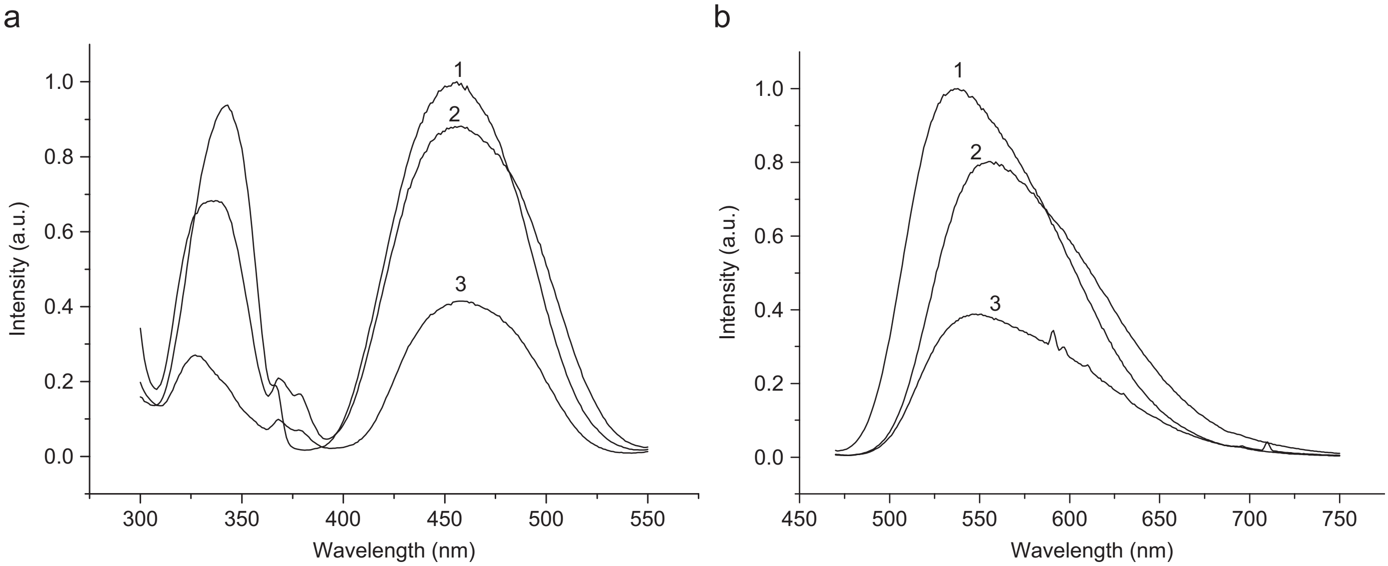

Fig. 2. Excitation (a) and emission (b) spectra of investigated samples $Tb_3Al_5O_{12}:Ce^{3+}$ (2) and double activated $Tb_3Al_5O_{12}:Ce^{3+}$, Eu^{3+} (3) with commercial $(YGd)_3Al_5O_{12}:Ce^{3+}$ (1).

the TAG sublattice, the Tb^{3+} in TAG acted both host and activator itself showing host lattice emission.

The comparison of the luminescence spectra of the TAG-based phosphors with the emission of the commercial YAG convinces us that the latter can serve as a very convenient reference material against which the emission efficiency of our phosphors can be judged. Since the emissions of all materials investigated fall within exactly the same spectral region, there is no need to correct the emission spectra for the photomultiplier response to make a reasonable calculation of the quantum efficiencies of the emissions of the various TAG powders. Reliable judgment of the real efficiencies of the emissions from the various specimens requires an accurate determination of the amount of light absorbed by each of the phosphors investigated. This is especially important in our case, since the various specimens are characterized by different microstructures and the activator concentration. To compare the amount of light absorbed by an actual specimen, we measured reflection spectra for each of them and related them to the reflectivity of our standard commercial YAG phosphor and to the reflectivity of MgO. Eq. (5) shows the relationship between the reflectance of the specimen investigated and the reflectance of the standard powder MgO.

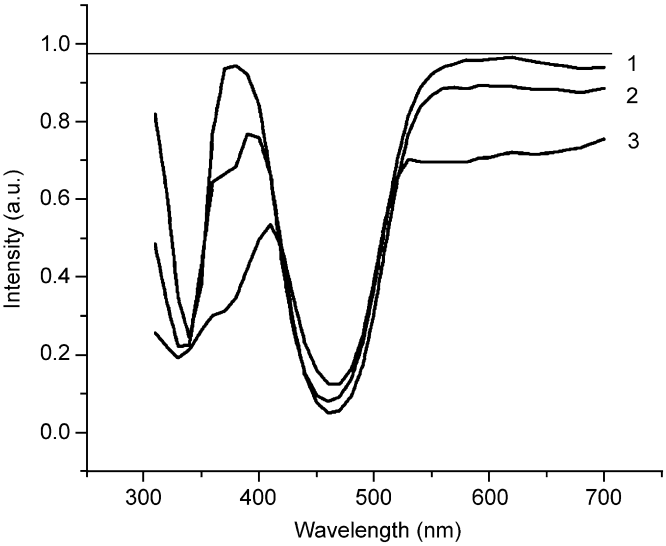

Fig. 3. Diffuse reflection spectra of the $Tb_3Al_5O_{12}:Ce^{3+}$ (2), double activated $Tb_3Al_5O_{12}:Ce^{3+}$, Eu^{3+} (3) and commercial $(YGd)_3Al_5O_{12}:Ce^{3+}$ (1) in comparison with MgO (straight line at 0.97).

In Fig. 3 we show reflection spectra for the commercial YAG and the TAG samples (one of them (2) is doped with 6 mol% of Ce^{3+} and other (3) with 3 mol% of Ce^{3+} and 3 mol% of Eu^{3+}), together with the spectrum of MgO. The results leave no doubt that, for reliable estimation of the quantum efficiency of an emission, it is definitely not enough to compare just the luminescence efficiency—it is also necessary to take into account the variations in the amounts of light absorbed by each of the samples. Despite the fact that all TAG specimens presented in Fig. 3 have the same host lattice, their capabilities for reflecting the incident light vary strongly. It can be explained by the different Ce^{3+} activator concentration in the samples (2) and (3), as well as influence of Eu^{3+} on the luminescence properties of the sample (3). Thus the amount of light accessible for absorption by the Ce^{3+} ions (able to excite the phosphor) must also alter. Generally, as expected, with rising Ce content (6 mol% in the sample 2 and 3 mol% in the sample 3) less and less light is being reflected, which means that a still increasing amount of the light is being absorbed by the phosphor.

On the basis of the excitation (Fig. 2) and reflection (Fig. 3) spectra, we decided that for the measurements of the quantum efficiencies of our phosphors, the most convenient excitation wavelength would be 460 nm. The diffuse reflection spectra at this wavelength is presented in the Fig. 4.

The quantum efficiency of phosphors calculated according to Eqs. (4) and (5) and by using the experimental data from Fig. 4, gives us the 76% for $Tb_3Al_5O_{12}$:Ce^{3+} (6 mol% Ce) and 40% for $Tb_3Al_5O_{12}$:Ce^{3+}, Eu^{3+} (3 mol% Ce and 3 mol% Eu). For comparison, the quantum efficiency of $(YGd)_3Al_5O_{12}$:Ce^{3+} is 90%. It is not astonishing, because the main reason of a low intensity of the last sample is a lack of Ce activator and weak emission intensity in comparison with standard sample. The quantum efficiency practically does not depend on excitation wavelength in the large excitation area. It is good as shown in Fig. 5 for our samples and could be explained by the same processes of energy absorption, energy transfer and emission at different excitations. The quantum efficiency strongly depends on the sample structure and activator concentration.

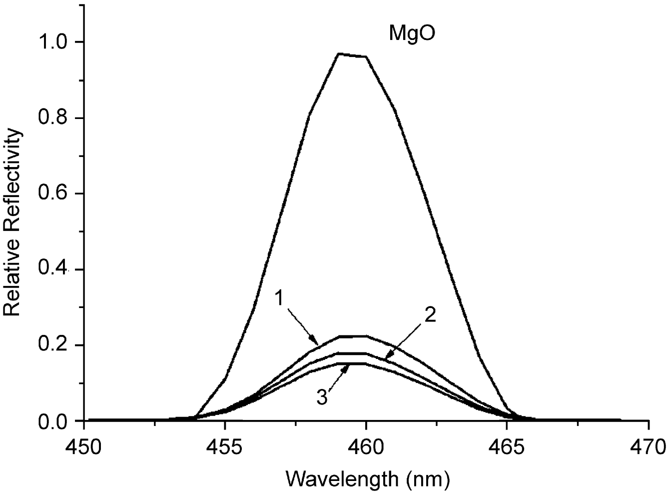

Fig. 4. Relative reflectivity of the $Tb_3Al_5O_{12}$:Ce^{3+} (2), double activated $Tb_3Al_5O_{12}$:Ce^{3+}, Eu^{3+} (3) and commercial $(YGd)_3Al_5O_{12}$:Ce^{3+} (1) in comparison with MgO at 460 nm excitation.

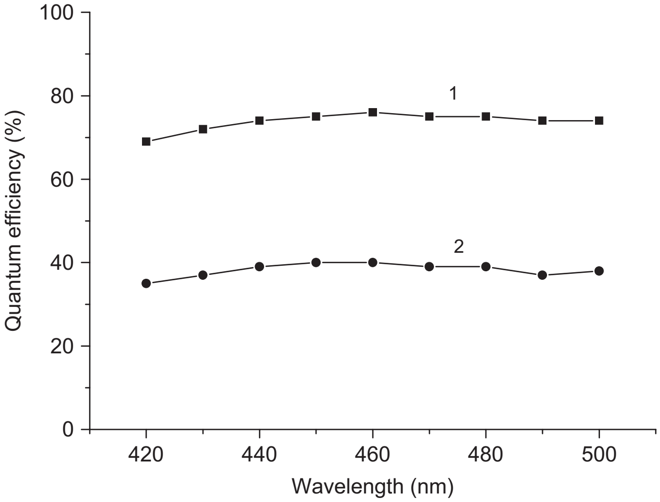

Fig. 5. The quantum efficiency of (1) $Tb_3Al_5O_{12}$:Ce^{3+} (6 mol% Ce^{3+}) and (2) $Tb_3Al_5O_{12}$:Ce^{3+}, Eu^{3+}(3 mol% Ce^{3+} and 3 mol% Eu^{3+}) in dependence of excitation wavelength.

Energy absorption need not necessarily take place at the activator ion itself but can occur at a random place in the lattice. This implies that energy transfer of the absorbed energy to the luminescent center takes place before emission can occur. The migration of the energy absorbed by the lattice can take place through one of the following processes:

- migration of electric charge (electrons, holes),
- migration of excitons,
- resonance between atoms with sufficient overlap integrals,
- reabsorption of photons emitted by another activator ion or sensitizer.

The occurrence of energy transfer within a luminescent material has far-reaching consequences for its properties as a phosphor. On the one hand the absorbed energy can migrate to the crystal surface or to lattice defects where it is lost by radiationless deactivation. As a consequence the phosphor energy yield, that is the quotient of emitted light energy to initially absorbed energy, drops. In the same phosphor structure with the same defect concentration the energy loss is also the same and emission is determined by the activator concentration.

Doping with 1–3–5 mol% Ce yields a broad-band $5d$–$4f$ Ce^{3+} luminescence. In addition to the direct Ce excitation we expect in double activated terbium aluminum garnet to see also the Eu contribution. Doping with 1 mol% Eu leads to a quenching of the Ce luminescence and to appearance of the Eu^{3+} luminescence due to the $^5D_0 \rightarrow {}^7F_J$ transitions of the Eu^{3+} ion, peaking at 591, 597, 610, 631, and 708 nm. The most intensive peak is allowed magnetic dipole $^5D_0 \rightarrow {}^7F_1$ transition. The relative intensity of Eu peak

(591 nm) in dependence of Eu and Ce concentration and quenching of the Ce luminescence are presented in Fig. 6.

From analysis of the experimental results one can conclude that the excitation of Eu occurs via the Ce quenching luminescence. It means that here there is an effect of the Ce^{3+} ion as a sensitizer for the Eu^{3+} luminescence. The Eu^{3+} luminescence can be also activated by a Tb^{3+} sensitizing, which is not too surprising as an energy transfer from Tb^{3+} to Eu^{3+} is well known in literature [10–13]. Therefore, the Tb^{3+} host lattice acts as a sensitizer for the activator Eu^{3+}, but also as an activator itself showing host lattice emission. The fluorescence of Tb^{3+} in the TAG is due to the transitions of the Stark components of the $^5D_4$ level to the Stark components of the ^7F_J levels, but the low energy excitation used in blue LED (460 nm) is not enough to excite these levels. The 227 nm excitation and more is needed to excite the host lattice. Nevertheless, one can expect the transfer of energy from

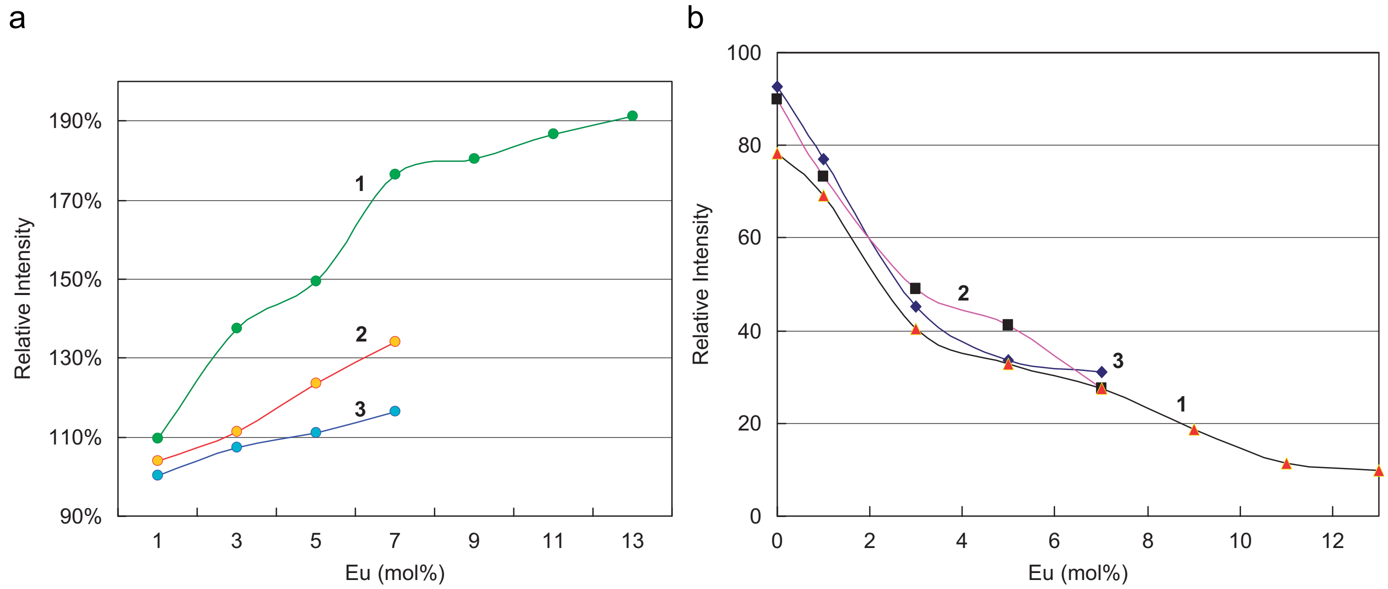

Fig. 6. (a) The relative intensity of Eu peak (591 nm) in dependence of Eu and Ce concentration and (b) quenching of the Ce luminescence: (1)-Ce 1 mol%; (2)-Ce 3 mol%; (3)-Ce 5 mol%.

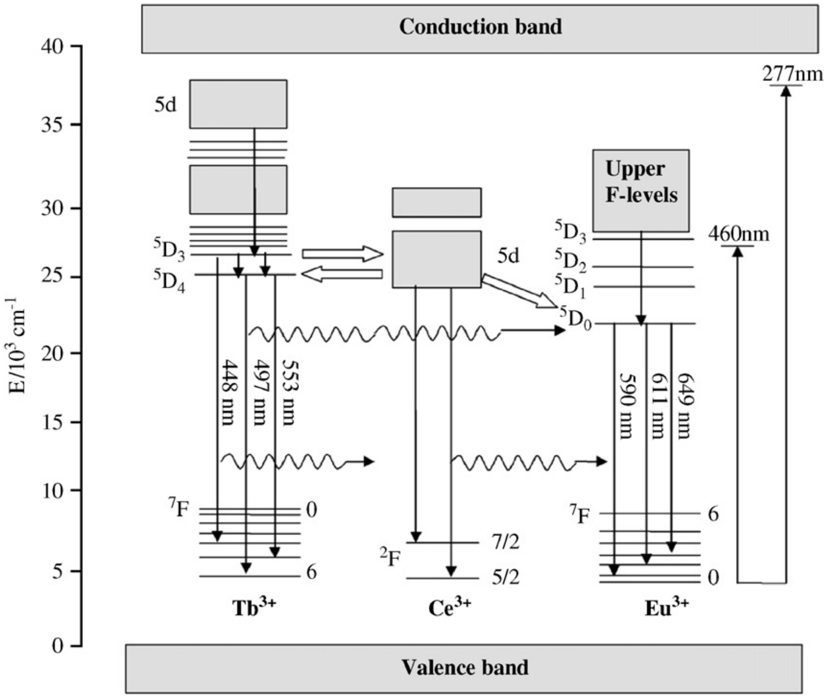

Fig. 7. Energy-level diagram and transfer pathways for Tb^{3+} and Ce^{3+} in TAG:Eu, Ce garnet.

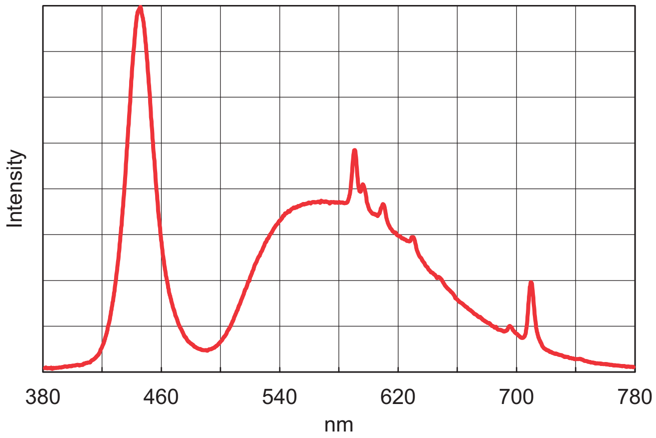

Fig. 8. Emission spectra of the blue LED including TAG:Ce, Eu.

the Ce^{3+} to Tb^{3+} lattice ion due to a slight overlap of the Ce^{3+} luminescence in TAG with the ${}^7F_6$–${}^5D_4$ absorption band of Tb^{3+} (483 nm). One more mechanism of Eu^{3+} luminescence is possible in this structure—it is direct excitation of 5*d* levels. But usually this luminescence is very weak, and only when upper *F*-levels are excited (at UV excitation), this luminescence becomes stronger.

In the TAG co-doped with Ce^{3+} and Eu^{3+}, the excitation into the Ce band at 460 nm leads to a Eu emission while in the case of the YAG lattice it does not [9]. This means that in TAG, Ce can be used as sensitizer, which transfers its energy via the Tb sublattice to the activator Eu. If this Tb sublattice is not available, such a sensitizing does not work.

The luminescence mechanism could be understood from the energy-level diagram (Fig. 7).

The first step of the path through which the activation energy is transferred from the sensitizer Ce to the activator Eu involves transfer between the $5d \rightarrow 4f\,{}^2F_{5/2;7/2}(Ce^{3+})$ and ${}^7F_6 \rightarrow {}^5D_4$ (Tb^{3+}) transitions. After migration in the Tb sublattice the activation energy is transferred from Tb^{3+} (${}^5D_4 \rightarrow {}^7F_J$) to a Eu^{3+} activator (${}^7F_J \rightarrow {}^5D_J$). Moreover, one additional way of transfer energy is possible: the radiation transitions in Tb may excite directly the neighboring Eu and Ce atoms. In such case, Tb^{3+} in TAG does not serve as a doping element but becomes a part of the host structure. After migration in the Tb sublattice the activation energy is transferred from Tb^{3+} (${}^5D_4 \rightarrow {}^7F_J$) to a Eu^{3+} activator (${}^7F_J \rightarrow {}^5D_J$). This part of the process was demonstrated for the single-doped case of TAG:Eu in [9]. In YAG, only a direct simultaneous excitation of Ce $^{3+}$ and Eu^{3+} at about 370 nm leads to a weak emission from both of the ions [9].

Application of cerium–europium double activated terbium aluminum garnet phosphor with improved luminescence properties in the light emitting device is demonstrated in Fig. 8.

Some additional Eu peaks and broadening the spectra in the red region significantly improves the color rendering index (CRI), CIE coordinates and luminescent properties of LED.

4. Conclusions

As discussed above, the $Tb_3Al_5O_{12}$ garnets co-activated with Ce^{3+} and Eu^{3+} are interesting materials in which radiative, nonradiative and energy-transfer processes can occur simultaneously at room temperature. The new LED-converter TAG doped with Ce and Eu has been investigated.

Simple express method of quantum efficiency measurement and calculation using PL spectroscopy system is proposed and the experimental scheme compatible with PL DARSA system is suggested.

The methodology of calculation quantum efficiency from reflection spectra is discussed. The obtained results show that the quantum efficiency only of an emission, it is definitely not enough to compare just the luminescence efficiency—it is also necessary to take into account the variations in the amounts of light absorbed by each of the samples.

In co-activated TAG:Ce, Eu the Tb^{3+} sublattice can sensitize the luminescence of both the Ce^{3+} and the Eu^{3+} ions. Moreover, even Ce^{3+} ions can transfer energy to Eu^{3+} ions, using the Tb lattice for the transport of the excitation energy. It is suggested that the energy is transferred from the sensitizer Ce via the Tb sublattice to Eu.

In order to get the better CRI and high efficiency in LED with double activated TAG:Ce, Eu very careful ratios between co-activators have to be chosen. Application of cerium–europium double activated terbium aluminum garnet phosphor in the light emitting device shows the better CRI and improved luminescence properties.

Acknowledgment

This work was partially supported by BK21 Program funded by the Ministry of Science and Technology of Korean government.

References

[1] S. Nakamura, M. Senob, N. Iwasa, S. Nagahama, T. Yamada, T. Mukai, Jpn. J. Appl. Phys. 34 (1995) L1332–L1338.
[2] S. Nakamura, M. Senob, N. Iwasa, S. Nagahama, Appl. Phys. Lett. 67 (1995) 1868–1872.
[3] P. Schlotter, J. Baur, C. Hielscher, M. Kunzer, H. Obloh, R. Schmidt, J. Schneider, J. Mater. Sci. Eng. B 59 (1999) 390–396.
[4] J. Yum, S. Seo, S. Lee, Y. Sung, J. Electrochem. Soc. 150 (2003) H47–H55.
[5] T. Tamura, T. Setomoto, T. Taguchi, J. Lumin. 87–89 (2000) 1180–1186.
[6] M. Nazarov, C. Yoon, J. Solid State Chem. 179 (2006) 2529–2533.
[7] G. Blasse, A. Bril, Appl. Phys. Lett. 11 (2) (1967) 53–58.
[8] W.J. Miniscalco, A.R. Pellegrino, W.M. Yen, J. Appl. Phys. 49 (1978) 6109–6115.

[9] M. Batentschuk, A. Osvet, G. Schierning, A. Klier, J. Schneider, A. Winnacker, Radiat. Meas. 38 (2004) 539–543.

[10] W.W. Holloway, M. Kestigian, R. Newman, Phys. Rev. Lett. 11 (10) (1963) 458–466.

[11] S.H. Park, S.I. Mho, K.W. Lee, Bull. Korean Chem. Soc. 17 (5) (1996) 487–491.

[12] M.V. Nazarov, D.Y. Jeon, J.H. Kang, E.-J. Popovici, L.E. Muresan, M.V. Zamoryanskaya, B.S. Tsukerblat, Solid State Commun. 131 (5) (2004) 307–311.

[13] M.V. Nazarov, B.S. Tsukerblat, E.J. Popovici, D.Y. Jeon, Solid State Commun. 133 (3) (2005) 203–208.